iScience

CellPress
OPEN ACCESS

Article

IDH1 K224 acetylation promotes colorectal cancer via miR-9-5p/NHE1 axis-mediated regulation of acidic microenvironment

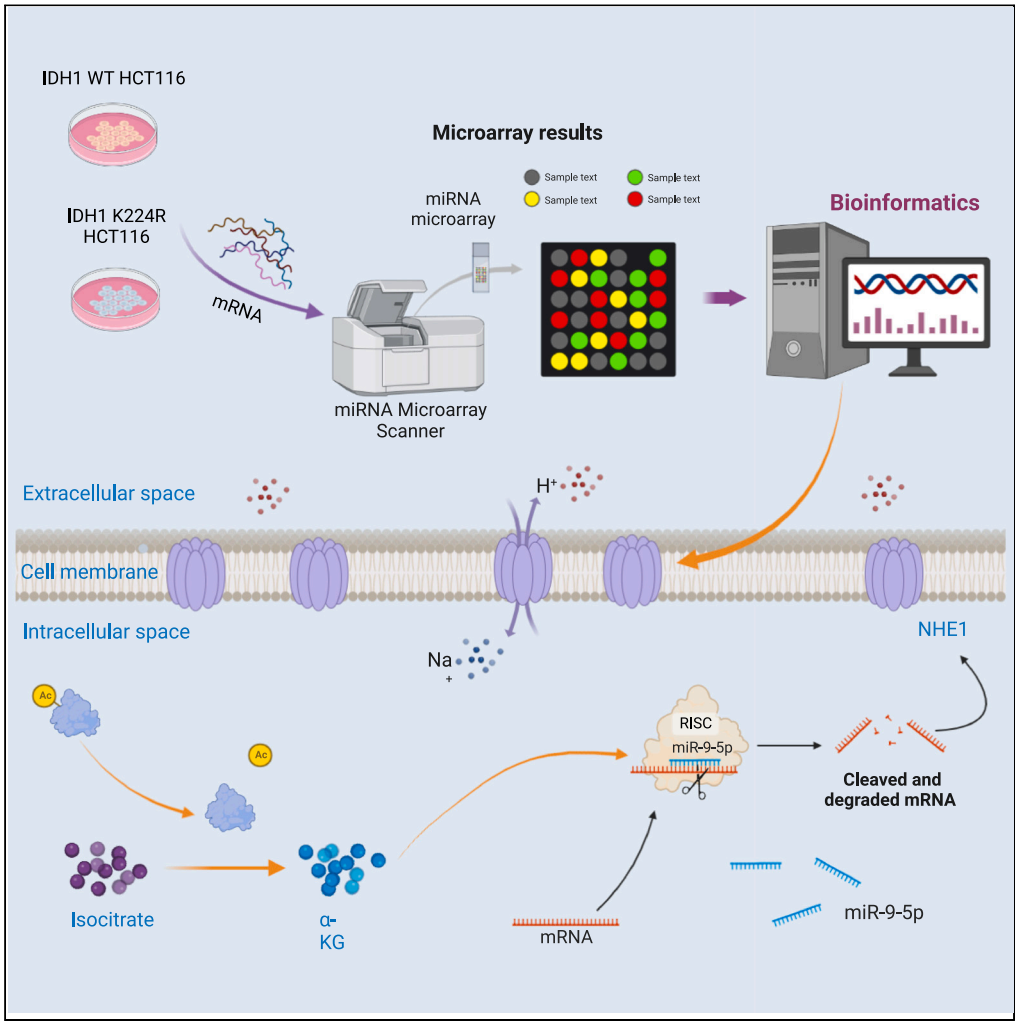

Bo Wang, Long Zhao, Changjiang Yang, ..., Yingjiang Ye, Jianyuan Luo, Zhanlong Shen

shenzhanlong@pkuph.edu.cn

Highlights

IDH1 hyperacetylation mediates the acidic microenvironment of colorectal cancer

α-KG can affect hydroxylation of Ago2 and mediates miR-9-5p targeting NHE1 protein

MiR-9-5p/Ago2/NHE1 axis regulates extracellular H^+ concentration

Wang et al., iScience 26, 107206
July 21, 2023 © 2023
https://doi.org/10.1016/j.isci.2023.107206

iScience

CellPress
OPEN ACCESS

Article

IDH1 K224 acetylation promotes colorectal cancer via miR-9-5p/NHE1 axis-mediated regulation of acidic microenvironment

Bo Wang,[1,3] Long Zhao,[1,3] Changjiang Yang,[1,3] Yilin Lin,[1] Shan Wang,[1] Yingjiang Ye,[1] Jianyuan Luo,[2] and Zhanlong Shen[1,4,*]

SUMMARY

The acidic microenvironment is considered an important factor in colorectal cancer (CRC) that contributes to malignant transformation. However, the underlying mechanism remains unclear. In a previous study, we confirmed that IDH1 K224 deacetylation promotes enzymatic activity and the production of α-KG. Here, we further investigate the effect of IDH1 hyperacetylation on the CRC acidic microenvironment. We demonstrate that increased α-KG affects hydroxylation of Ago2 and mediates miR-9-5p targeting NHE1 protein. Knockdown of NHE1 dramatically attenuates CRC cell proliferation and migration by restricting transport of intracellular H^+ out of cells. Furthermore, we show that miR-9-5p is the microRNA with the most significant difference in the alteration of IDH1 K224 acetylation and can downregulate NHE1 mRNA. Our data also indicate that hydroxylation stabilizes Ago2, which in turn promotes miR-9-5p activity. Taken together, our results reveal a novel mechanism through which IDH1 deacetylation regulates the cellular acidic microenvironment and inhibits CRC metastasis.

INTRODUCTION

Colorectal cancer (CRC) is a common malignant tumor that poses a serious threat to human health.[1] Distant metastasis—especially liver metastasis—is an important cause of poor prognosis in CRC patients.[1,2] However, the molecular mechanisms underlying metastasis of CRC remain unclear.

Hypoxia around solid tumors can induce metabolic transformation of cells. Tumor cells are forced to provide energy by glycolysis rather than oxidative phosphorylation, which eventually become permanent even in aerobic conditions; this phenomenon is termed the "Warburg effect."[3] To maintain a normal pH value in cells, the Na^+/H^+ exchanger (NHE) and proton pump inhibitor (PPI) on the tumor cell membrane must constantly transport intracellular H^+ out of cells.[4,5] De Milito et al. demonstrated that the ability of PPI to inhibit tumor cells is directly related to acidity of the medium.[6] Downregulation of NHE1 has also been shown to significantly inhibit the invasion and metastasis of glioma cells.[7] Thus, the invasive capabilities of tumor cells are closely associated with metastasis and altering pH seems to affect tumor cell metastasis.

Protein post-translational modification (PTM), especially lysine acetylation, affects cell growth and progression. In a previous screening study using proteomics methods, we identified acetylation of IDH1 at the lysine 224 site as playing a key role in CRC metastasis.[8] IDH1 is an $NADP^+$-dependent enzyme located in the cytoplasm that converts isocitrate to α-ketoglutarate (α-KG), thereby greatly affecting the tricarboxylic acid cycle (TAC).[9] When the TAC is impaired, pyruvic acid transforms to lactic acid to result in an intracellular acidic environment. To maintain homeostasis, cancer cells must pump out H^+ to accelerate the extracellular acidic environment.[10] Cells generally eliminate their metabolic acid load via membrane proteins that mediate H^+ extrusion (e.g., Na^+/H^+ exchange, H^+-ATPase activity) or $HCO3^-$ uptake (e.g., Na^+, $HCO3^-$ cotransporter NBCnl).[11] In CRC, Na^+/H^+ exchanger 1 (NHE1) is reported to regulate intracellular pH in relation to the tumor microenvironment[12] and is a potential target of cisplatin that could increase cell sensitivity to chemotherapy.[13] Thus, we speculate that IDH1 acetylation may regulate H^+ extrusion via α-KG. However, the mechanism is unknown.

[1]Department of Gastroenterological Surgery, Laboratory of Surgical Oncology, Beijing Key Laboratory of Colorectal Cancer Diagnosis and Treatment Research, Peking University People's Hospital, No.11 Xizhimen South Street, Beijing 100044, P.R. China

[2]Department of Medical Genetics, Peking University Health Science Center, Beijing 100191, P.R. China

[3]These authors contributed equally

[4]Lead contact

*Correspondence: shenzhanlong@pkuph.edu.cn

https://doi.org/10.1016/j.isci.2023.107206

This is an open access article under the CC BY-NC-ND license (http://creativecommons.org/licenses/by-nc-nd/4.0/).

Qi et al. found that α-KG along with proline hydroxylase (PHD) hydroxylates Ago2 to stabilize Ago2 expression.[14] Ago2 is a key part of the RNA-induced silencing complex (RISC) complex that regulates microRNA (miRNA) expression or production. Subsequently, miRNA and RISC form a complex to regulate the mRNA expression of downstream genes.[15] As an important PTM, hydroxylation plays a crucial role in the biological processes of cells. Mass spectrometry has shown that endogenous Ago2 is hydroxylated at the 700th proline, and mutation of proline to alanine at this site causes instability of Ago2.[14] In this way, regulation of the 700th proline residue by hydroxylation is linked to stability. This finding suggests that hydroxylation as a PTM is important for Ago2 stability and effective miRNA interference.[14]

In recent years, it has been found that production of miR-451 does not require the Dicer enzyme, whereas Ago2 is necessary.[16] miRNAs are the most comprehensively and extensively studied endogenous non-coding RNA. They are widely involved in regulation of the tumor acidic microenvironment and regulated by protein acetylation modification, which further affects tumor invasion and metastasis.[17–21] Although many studies have reported the functions of various miRNAs in CRC, there is still a lack of understanding of how specific miRNAs affect biological pathways and outcomes.[22] Indeed, in CRC, whether IDH1 acetylation regulates H^+ extrusion via the Ago2/miRNA pathway remains unclear.

In a previous study, we demonstrated that SIRT2 deacetylated IDH1 at K224 and exhibited a tumor suppression function in a colon cancer cell model through IDH1 enzymatic activities. Deacetylation of IDH1 K224 by SIRT2 significantly inhibited the malignant behaviors of CRC cells *in vitro* and *in vivo* and predicted poor survival in CRC patients.[23] In the present study, we investigated the function of IDH1 K224 acetylation in the regulation of the extracellular acidic microenvironment. We found that deacetylation of IDH1 K224 upregulated α-KG to affect hydroxylation of Ago2 and mediated miR-9-5p targeting NHE1 protein. These findings may provide new insights for IDH1 acetylation-dependent extracellular acidic microenvironment treatment of liver metastasis in CRC.

RESULTS

IDH1 mRNA and protein expression levels in CRC patients

Consistent with the results of our previous study, the mRNA and protein expression levels of IDH1 in colorectal cancer are significantly lower than those in normal tissues (Figures S1A–S1C). Regarding IDH1 protein expression in CRC, we found that immunohistochemical analysis of IDH1 was negative in CRC but positive in normal tissues (Figure S1D), as were other tumors (Table S1). The results in the Cancer Genome Atlas (TCGA) database showed that the median survival time was higher in patients with IDH1 high-expression group compared with low-expression group, but this difference was not statistically significant (Figure S2A). Moreover, data analytics in TCGA showed that the expression of IDH1 was directly proportional to the number of Th2 cells infiltrating in the immune microenvironment and inversely proportional to Th1 cells (Figure S1E).

Acidic microenvironment impacts CRC functions *in vitro*

To explore the effect of an acidic microenvironment on CRC cells, we cultured culture the colon cancer cell lines SW480 and HCT116 in media of different pH values and then evaluated cell proliferation, invasion, and migration ability. As the pH value of the medium gradually decreased from 7.4 to 6.6, the proliferation ability of the SW480 and HCT116 cells significantly increased. However, when the pH value continued to drop to 6.2, the number of invasive cells decreased (Figures 1A and 1B). Consistently, the pH value of the culture medium also impacted CRC cell migration (Figures 1C and 1D) and promoted its colony formation within a certain range (Figures 1E and 1F).

IDH1 K224 acetylation is involved in regulation of the acidic microenvironment of CRC cells

Our previous research has revealed that IDH1 deacetylation represses CRC cell invasion and migration, here, we see in the Compendium of Protein Lysine Modifications 4.0 (CPLM 4.0) database, the acetylation on K224 of IDH1 may be an important one among many acetylation sites (Figure S1F). Conservation analysis of IDH1 indicated that K224 is a highly conserved site from Danio rerio to Homo sapiens (Figure S1G). And in order to clarify whether IDH1 acetylation of K224 affects the cell acidic microenvironment, we constructed a wild type (WT) IDH1 plasmid and mutant plasmid. In the IDH1 mutant plasmid, the lysine site (K) was muted to arginine (R) to mimic the deacetylated states of protein while K to glutamine (Q) presented the acetylated situation. The WT IDH1 plasmid and IDH1 K224R plasmid were transfected

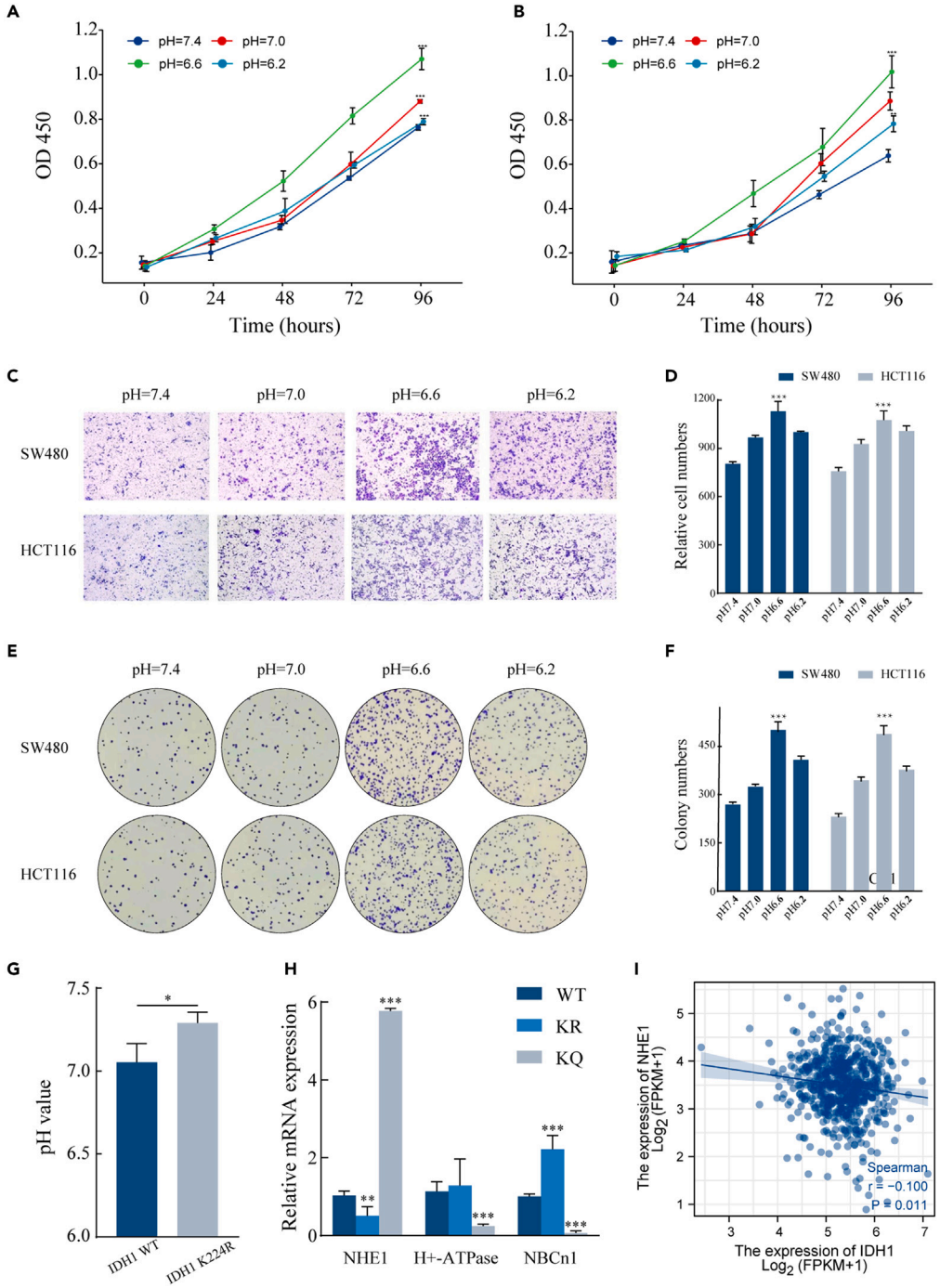

Figure 1. The expression of IDH1 in CRC and its acetylation regulates the acidic microenvironment

(A and B) Colony formation ability after changing the pH of culture medium.

(C and D) Transwell assay was performed to evaluate the invasion abilities of SW480 and HCT116 cells after setting the culture medium to different pH values. Stained cells in the lower chambers were quantified.

(E and F) CCK8 assay showing cell proliferation of SW480 and HCT116 cells in different pH value culture medium.

(G) Extracellular pH assessed by pH meter in HCT116 cells after overexpression of IDH1 wild type or K224R plasmid.

(H) Relative mRNA expression of different transporters that regulate H^+ in WT, K224R, K224Q cells.

(I) Correlation between IDH1 and NHE1 expression in TCGA database.

into IDH1 knockout HCT116 cells. As shown in Figure 1G, the medium of K224R cells had a significantly higher pH value than that of the WT cells, indicating that acetylation of the K224 site of IDH1 affected the acidic microenvironment.

The expression of NHE1 is affected by IDH1 acetylation

IDH1 activity may result in the accumulation of acidic metabolites in cells; however, as cells can eliminate metabolic acid load via H^+ extrusion, the mechanism requires clarification. We analyzed the mRNA expression of membrane proteins regulating the acidic metabolism of cells, including NHE1, H^+-ATase, and NBCnl. The mRNA expression of NHE1 altered more obviously than H^+-ATPase and NBCnl in different IDH1 K224 acetylation levels HCT116 cells (Figure 1H). Also, the data from the TCGA showed that the mRNA expression levels of IDH1 and NHE1 were significantly negatively correlated (Figure 1I).

NHE1 regulates cell invasion and migration by regulating extracellular pH

Initially, we used TCGA databases to compare the transcription levels of NHE1 in many types of cancer and normal individuals. The NHE1 mRNA expression was increased in a variety of malignant tumors, but the opposite is true in CRC (Figure S2G). Supplementary 2B to 2E showed that five-year survival rates were higher in glioblastoma, lower grade glioma, liver cancer and mesothelioma patients with NHE1 low-expression group compared with high-expression group. To verify the effect of NHE1 on the extracellular acidic microenvironment and the biological behaviors of CRC cells, we knocked down NHE1 in HCT116 cells. The efficiency of siRNAs was confirmed by western blot and quantitative real-time polymerase chain reaction (qRT-PCR). As si-2 showed higher interference efficiency than si-1, it was selected for the subsequent experiments (Figures 2A and 2B). The migration and invasion abilities of HCT116 and SW480 cells were obviously decreased after NHE1 knockdown by si-2 (Figures 2C–2F). When the culture time increased from 12 h to 36 h, the pH of the cell culture medium gradually declined in both HCT116 and SW480 cells; however, the decline rate was lower in CRC cells in the groups with NHE1 knocked down (Figure 2G). Furthermore, the pH values in NHE1 knockdown cells were significantly higher than those in control cells at the same culture time. Through bioinformatics analysis, we found that the expression of NHE1 was highly positively correlated with NK CD56 bright cells (Figure S2H). In addition, through GO and KEGG analysis, we found that the differential genes between the NHE1 high-expression group and the low-expression group were mainly enriched in nucleosome assembly, nucleosome, serine-type endopeptidase inhibitor activity, and systemic lupus erythematosus (Figure S2I).

IDH1 acetylation affects the expression of miRNA in CRC cells

To investigate the mechanism through which IDH1 K224 acetylation regulates the acidic microenvironment in CRC, we used Agilent miRNA chips for miRNA screening. We identified 50 miRNAs with more than 2-fold differential expression between WT cells and K224R cells: of these, 44 miRNAs were upregulated and 6 miRNAs were downregulated (Table 1). We used the TAM2.0 Website tools to compare these differential miRNAs, which collapse the mature miRNA names provided to the corresponding miRNA genes. We chose cancer-related miRNA sets to constitute the major part of our curated data. The results are shown in Figure 3A. As can be seen, most of these differential miRNAs have been linked to various cancers, including CRC. Figure 3B shows the diseases enriched by miRNAs with the largest fold differences, with the blue and red bars representing downregulated and upregulated miRNAs, respectively. As shown, some of the upregulated miRNAs with the largest fold differences are positively correlated with the occurrence of rectal cancer.

Next, we used the bioinformatics software TargetScan 7.1 to predict miRNAs that may regulate NHE1 expression. Both the bioinformatics prediction approach and microarray screening results identified miR-9-5p. Notably, miR-9-5p showed the greatest differential expression among all candidates screened using miRNA chips, showing more than 5-fold upregulation (Figure 3B). Enrichment analysis was performed on all target genes of miR-9-5p. As shown in Figure S3A, the results indicate that these genes are enriched in the KEGG pathway of "response to oxygen levels" and "response to decreased oxygen levels." Since some pathways are related to lymphocytes, we further employed bioinformatics methods to analyze the correlation between miR-9-5p and various lymphocytes. As shown in Supplementary 1D, the expression of miR-9-5p was significantly positively correlated with Gamma delta (γδ), T cells, B cells, Mast cells, and NK cells, but negatively correlated with the number of Th2/Th17 cells (Figure 3D).

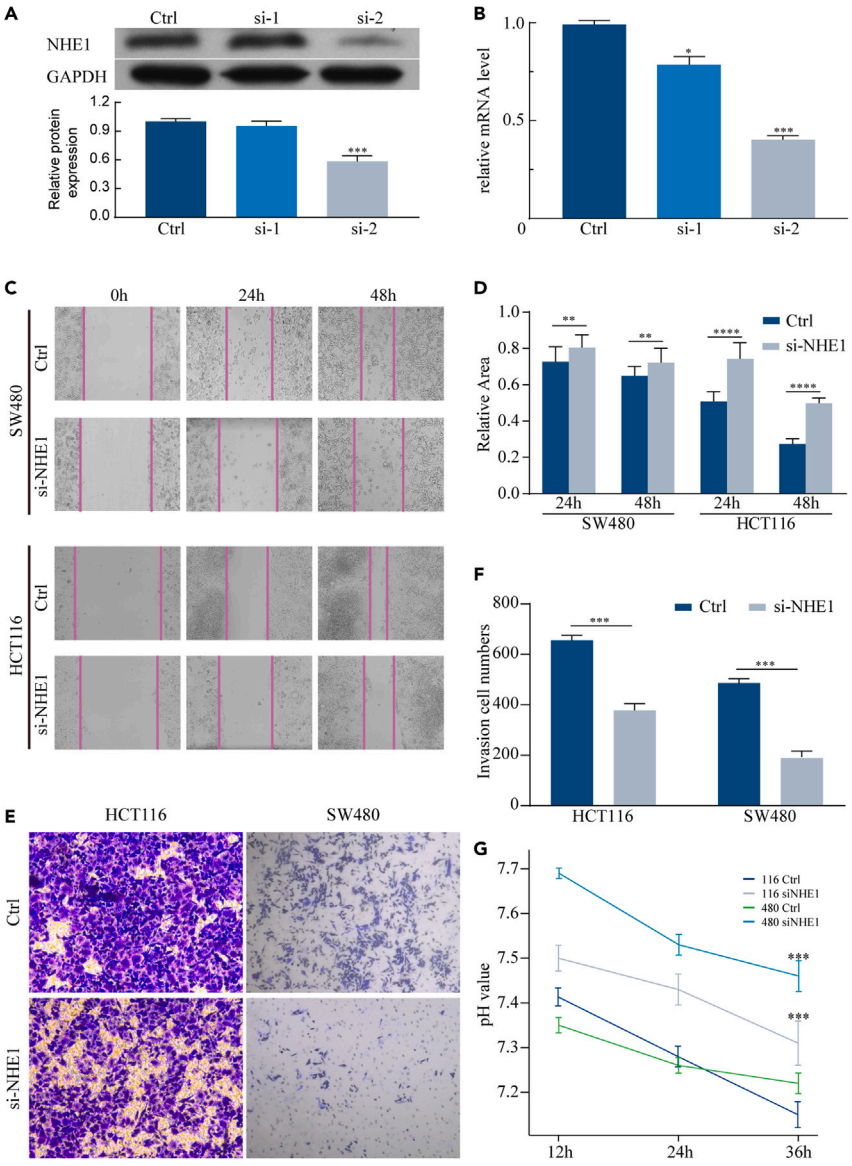

Figure 2. Knockdown of NHE1 inhibits HCT116 and SW480 cells invasion, migration and extracellular pH

(A and B) Western blot and qRT-PCR showed that NHE1 was downregulated in colorectal cancer cells after transfection of siRNAs.

(C and D) Wound healing assay was performed on HCT116 and SW480 cells treated with siRNAs or siNC (Ctrl). The area was measured at the indicated time points.

(E and F) HCT116 and SW480 cells were treated with siRNAs or siNC (Ctrl) for 48 h. Transwell assay was performed to evaluate the invasion abilities of HCT116 and SW480 cells. Stained cells in the lower chambers were quantified.

(G) NHE1 suppression inhibited the extracellular pH of HCT116 and SW480 cells.

IDH1 acetylation affects NHE1 expression via regulation of miR-9-5p

To test the hypothesis that miR-9-5p directly targets NHE1, we first transfected miR-9-5p mimics into SW480 cells. The expression of NHE1 mRNA and protein was significantly downregulated (Figures 4A and 4B), indicating that miR-9-5p can inhibit the expression of NHE1. The invasion and proliferation capacity of SW480 cells was also attenuated by upregulation of miR-9-5p (Figures 4C–4F). Subsequently, qRT-PCR was used to assess the expression of miR-9-5p and NHE1 in cells with different acetylation levels, including WT, K224R, and K224Q cells. The results showed that miR-9-5p expression was downregulated while NHE1 expression was increased (both $p < 0.05$) in K224Q cells, whereas the results in K224R cells

Table 1. Differential miRNA screened by Agilent miRNA chip

miRNA	p value	fold change	Correlation p value	K224R/WT
hsa-miR-9-5p	3.96E-08	5.0266385	6.43E-07	up
hsa-miR-424	1.61E-07	4.790935	1.74E-06	up
hsa-miR-96	1.88E-05	4.6753187	9.50E-05	up
hsa-miR-224	1.19E-09	4.0992484	6.76E-08	up
hsa-miR-193a-3p	2.46E-11	3.8018782	1.86E-09	up
hsa-miR-374a	9.63E-08	3.6398978	1.23E-06	up
hsa-miR-18a	1.60E-07	3.405375	1.74E-06	up
hsa-miR-374b	1.03E-07	3.2578483	1.24E-06	up
hsa-miR-18b	6.33E-08	3.241428	8.98E-07	up
hsa-miR-642b	4.63E-05	3.1707356	2.10E-04	up
hsa-miR-494	3.82E-06	3.1002054	2.48E-05	up
hsa-miR-17	1.58E-08	3.0253882	2.98E-07	up
hsa-miR-874	1.64E-06	2.8921137	1.16E-05	up
hsa-miR-574-5p	2.63E-07	2.872613	2.51E-06	up
hsa-miR-575	2.69E-07	2.8667836	2.51E-06	up
hsa-miR-214	3.97E-07	2.7780242	3.47E-06	up
hsa-miR-199b-5p	5.19E-06	2.7233331	3.16E-05	up
hsa-miR-30b	1.71E-06	2.6923351	1.17E-05	up
hsa-miR-296-5p	4.63E-08	2.6503394	7.00E-07	up
hsa-miR-425	3.12E-04	2.608453	0.001106846	up
hsa-miR-497	6.81E-07	2.5956757	5.52E-06	up
hsa-miR-582-5p	9.07E-04	2.5721729	0.002644529	up
hsa-miR-663	2.48E-08	2.5235507	4.33E-07	up
hsa-miR-10b	4.11E-05	2.5190513	1.90E-04	up
hsa-miR-99b	3.53E-04	2.5041425	0.001196308	up
hsa-miR-181a	2.10E-05	2.4961073	1.04E-04	up
hsa-miR-103	7.84E-06	2.4097784	4.45E-05	up
hsa-miR-27b	1.07E-08	2.3861763	2.42E-07	up
hsa-miR-301a	1.72E-05	2.2875125	9.09E-05	up
hsa-miR-101	4.37E-04	2.269115	0.001398463	up
hsa-miR-590-5p	2.20E-04	2.223755	8.34E-04	up
hsa-miR-188-5p	6.43E-07	2.1704097	5.41E-06	up
hsa-miR-29c	6.76E-04	2.1453586	0.002045042	up
hsa-miR-451	1.65E-04	2.1434171	6.81E-04	up
hsa-miR-125a-3p	8.15E-04	2.140921	0.002434763	up
hsa-miR-200c	1.43E-05	2.1153274	7.93E-05	up
hsa-miR-141	0.002199963	2.1135263	0.005740133	up
hsa-miR-151-5p	3.94E-04	2.1107652	0.001316055	up
hsa-miR-125a-5p	1.68E-05	2.1066935	9.09E-05	up
hsa-miR-125b	0.004796712	2.099044	0.010780729	up
hsa-miR-1	6.33E-04	2.0902555	0.00194311	up
hsa-miR-429	1.09E-06	2.0666552	8.56E-06	up
hsa-let-7g	1.16E-06	2.0383909	8.59E-06	up
hsa-miR-140-3p	3.07E-05	2.0094886	1.46E-04	up
hsa-miR-4281	0.002030803	4.1526136	0.005360376	down

(*Continued on next page*)

Table 1. *Continued*

miRNA	p value	fold change	Correlation p value	K224R/WT
hsa-miR-4299	0.008836888	2.1870918	0.018403428	down
hsa-miR-99a	0.005613912	2.1439571	0.012372408	down
hsa-miR-365	0.002819073	2.141723	0.006880964	down
hsa-miR-376a	2.84E-04	2.0393367	0.001022722	down
hsa-miR-192	0.001349537	2.015111	0.00382931	down

were the opposite (Figure 4G). Similarly, the acid-base of the culture medium had also changed after transfecting miR-NC or miR-9-5p mimic into CRC cells (Figure 4H).

Furthermore, we used TargetScan to analyze the possible binding sites between miR-9-5p and NHE1. The results showed that the binding sites of miR-9-5p and NHE1 are relatively conserved across different species (Figure S3B). The binding sequences between NHE1 and miR-9-5p are shown in Figure S3B using TargetScan Human 7.2. We also designed a mutated binding sequence (Figure 5A). The results of the dual-luciferase reporter assay showed that miR-9-5p expression significantly attenuated the luciferase activity of the reporter with the WT NHE1 promoter, but not that with the mutant reporter (Figures 5B and 5C).

IDH1 K224 acetylation level is correlated with the expression of Ago2 and NHE1 protein in CRC cells and tissues

Ago2 is a crucial partner of miRNAs in regulating the expression of target RNA. The results of the RNA co-immunoprecipitation assay with flag-tagged Ago2 showed that the level of miR-9-5p bound to Ago2 in K224R cells was significantly higher than that in WT and K224Q cells (Figure 5D and Table S2). To further investigate the relationship between the expression levels of Ago2 and acetylation modification of IDH1, we determined Ago2 expression among K224R, K224Q, and WT cells. As shown in Figure 5E, Ago2 expression in K224R cells was significantly higher than that in the other cells. The previous results were also confirmed by repeated experiments in SW480 cells (Figures S5A–S5C).

The immunohistochemistry results revealed that IDH1 K224 acetylation, Ago2 protein, and NHE1 protein were mainly expressed in the cytoplasm of CRC tissues. Compared to normal tissues, 52% (26/50), 48% (24/50), and 58% (29/50) of the CRC tissue samples showed high IDH1 224 acetylation, Ago2, and NHE1 positive expression, respectively. Moreover, the IDH1 K224 acetylation level was significantly correlated with NHE1 expression ($p < 0.05$); however, no significant correlation with Ago2 expression ($p > 0.05$) was observed in the 50 CRC tissue samples (Figure 5F).

IDH1 acetylation stabilizes Ago2 protein expression by enhancing hydroxylation

As previous study reported that α-KG, a substrate of IDH1, could stabilize Ago2 expression by hydroxylating Ago2,[10] we speculated that acetylation modification of IDH1 might influence the regulation of Ago2 through a similar mechanism. To assess this hypothesis, we quantified the α-KG content in the medium of WT and K224R HCT116 cells. After 24 h and 48 h of culture, α-KG was significantly increased in the medium of K224R cells compared to WT cells (Figure 5G). Furthermore, after α-KG was added to the medium of HCT116 cells (Figure 5H), the expression of Ago2 increased whereas the expression of NHE1 decreased. When we added α-KG to WT/K224R/K224Q stable cells, we observed that the expression of NHE1 changed, and the pH value in the medium also changed (Figures 5I–5K). At the same time, a number of cellular tumor biological assays of WT/K224R/K224Q stable cells showed that the cancer-promoting effect of IDH1 K224 acetylation was counteracted when α-KG was added to the cell culture medium (Figures S4A–S4H). While, the expression of IDH1, miR-9-5p, and NHE1 did not change when we changed the pH of the medium only (Figures S5D and S5E). In order to exclude the effect of α-KG alone on the pH of the medium, we added α-KG directly to the cell-free medium, and the results showed that the pH did not change with the addition of α-KG (Figure S5F).

The proline hydroxylase (PHD) detection kit was used to test PHD activity in K224R, K224Q, WT, and blank vector transfection cells. Compared to WT cells, PHD activity (optical density [OD] value at 450 nm) was significantly enhanced in K224R cells, but decreased in K224Q cells (Figure 6A). The co-immunoprecipitation results

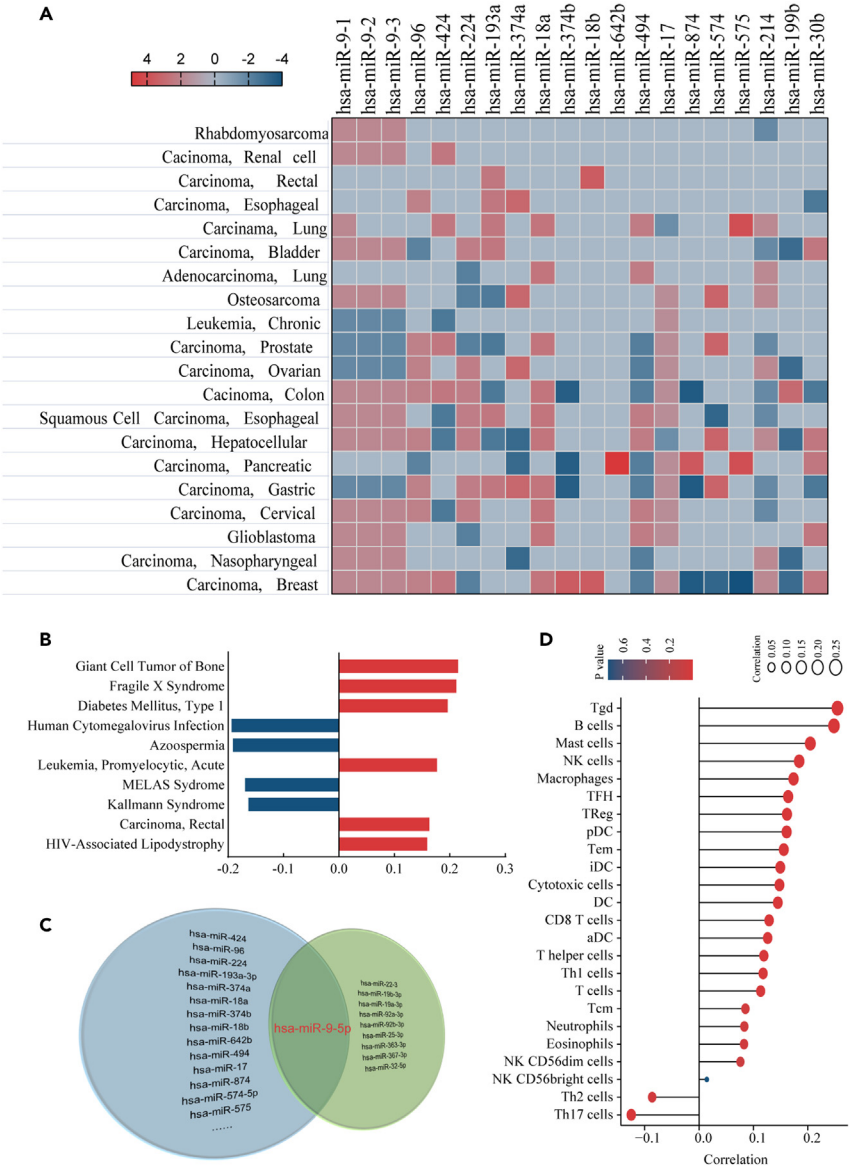

Figure 3. Bioinformatics analysis of differential miRNAs

(A) Heatmap of correlations between differential miRNAs and different cancers.

(B) Correlation analysis between up/downregulated top fifteen differential genes and different diseases.

(C) The miRNA in the green circle regulate NHE1 and the differential miRNA between IDH1 K224R and WT screened by Agilent miRNA chips were in the blue circle. The Venn diagram shows that the miRNA shared by the two groups is miR-9-5p.

(D) Correlation between miR-9-5p and immune cells around tumors in TCGA database.

showed that the hydroxylation level of Ago2 was clearly higher in K224R cells compared to the other cells (Figure 6B).

Furthermore, the cycloheximide (CHX) chase assay was used to determine the effect of hydroxylation on Ago2 stability. The Ago2-FLAG plasmid was transfected into K224R and WT cells, and CHX was added to inhibit the function of ribosomes at 3 h, 6 h, and 9 h after transfection. The Ago2 protein was enriched by immunoprecipitation to observe its degradation rate. The results showed that Ago2 protein expression at 6 h and 9 h in IDH1 K224R cells was higher than that in WT cells (Figure 6C), indicating that the protein stability of Ago2 increased and the half-life was prolonged in K224R cells. Since P700 was confirmed to be

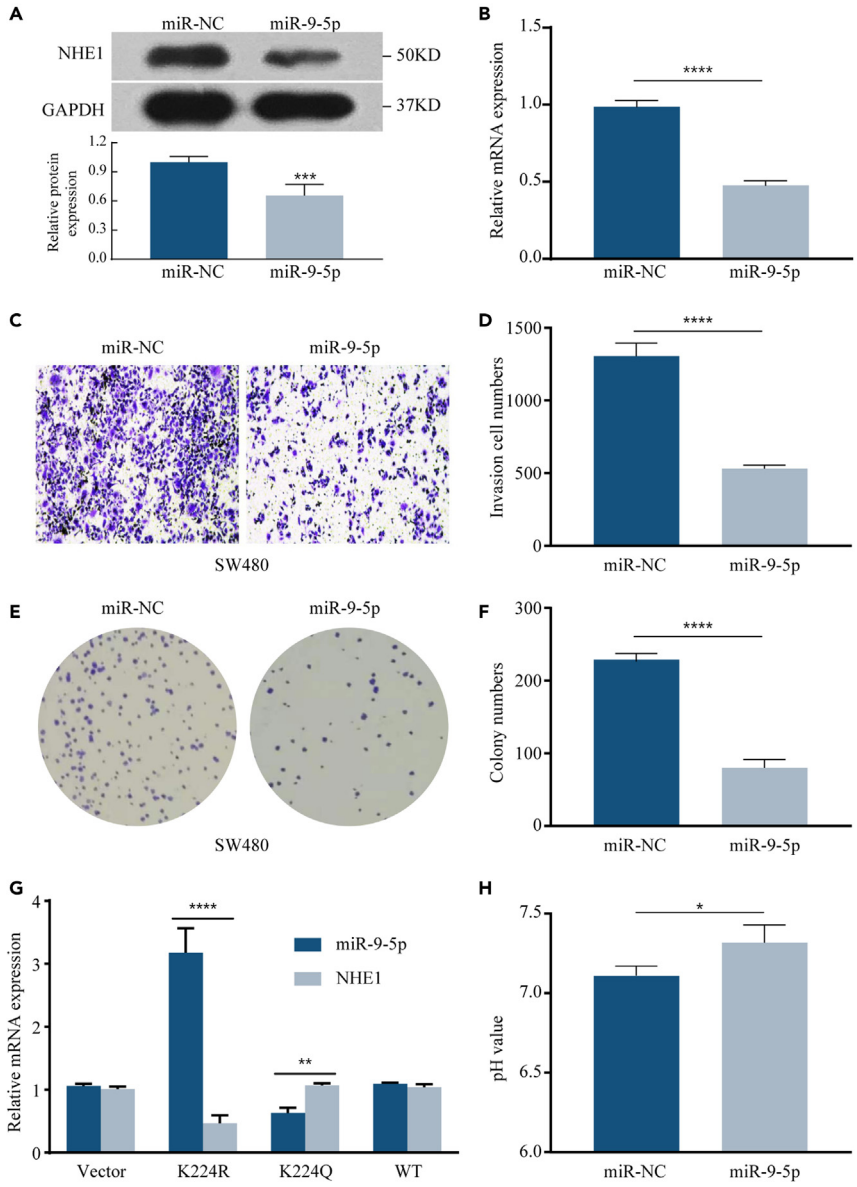

Figure 4. miR-9-5p down-regulates NHE1 in colon cancer cells

(A and B) Western blot and qRT-PCR showed that NHE1 was downregulated in colorectal cancer cells after transfection of miR-9-5p.

(C and D) Transwell assay was performed to evaluate the invasion abilities of SW480 cells after transfection of miR-9-5p.

(E and F) Colony formation ability after transfection of miR-NC and miR-9-5p mimic.

(G) Mutation of IDH1 K224R and K224Q causes altered mRNA levels of NHE1 and miR-9-5p measured by RT-qPCR.

(H) Alternation of the medium pH value after transfection of miR-NC and miR-9-5p mimic.

the main hydroxylation site of Ago2, it was mutated to investigate the effect on the ubiquitination of Ago2; ubiquitination is the main degradation pathway of Ago2 protein.[24,25] As shown in Figure 6D, ubiquitination of Ago2 was obviously enhanced after the hydroxylation of Ago2 was inhibited.

IDH1 K224 deacetylation impairs CRC growth and affects the expression of Ago2 and NHE1 *in vivo*

To gain further insights into the physiologic significance of IDH1 hypoacetylation on CRC progression, we established a xenograft tumor model in nude mice injected with Vector, IDH1 WT, IDH1 K224Q, or IDH1

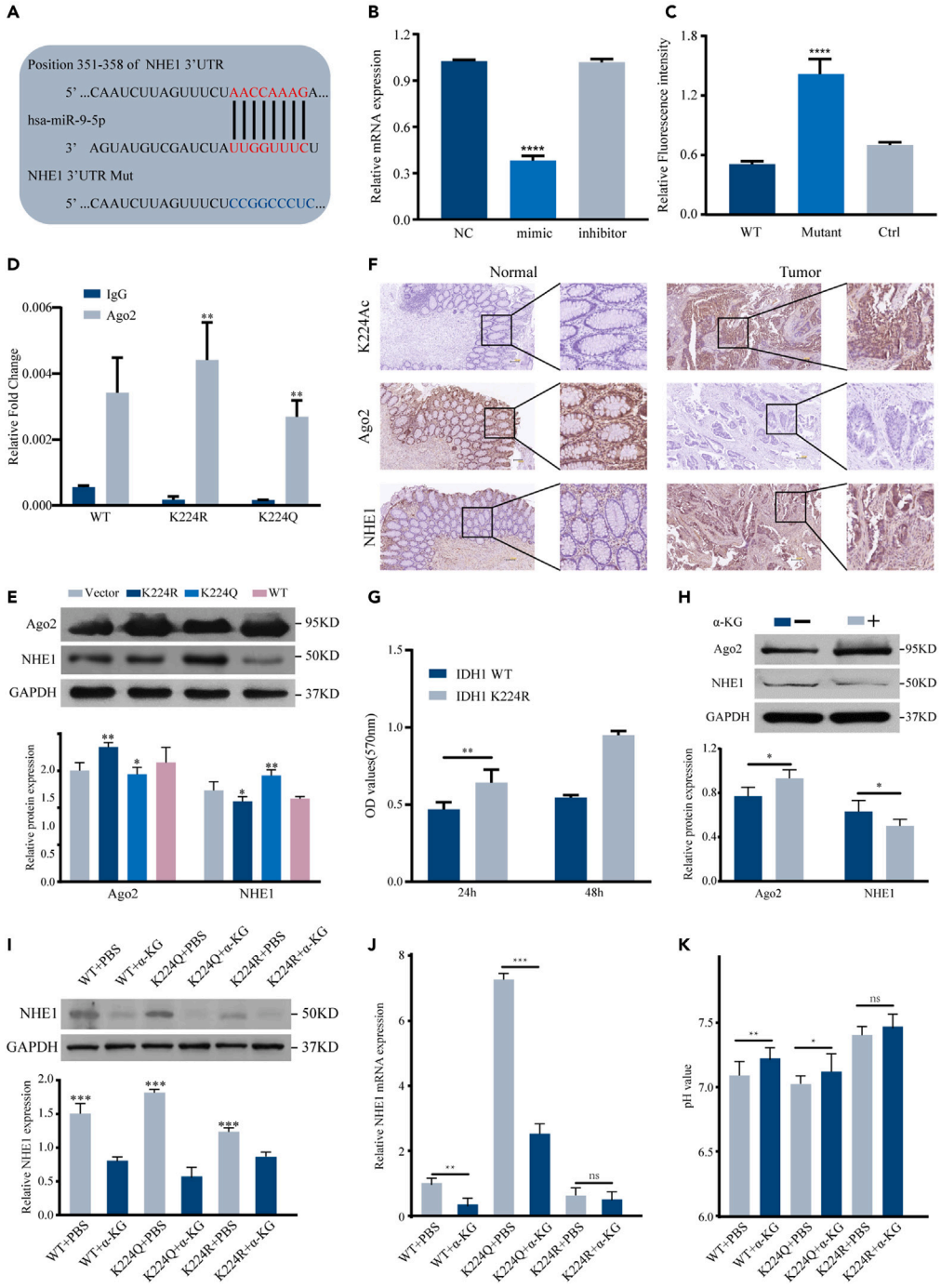

Figure 5. The effect of IDH1 acetylation on miR-9-5p and NHE1

(A) The mRNA level of NHE1 were analyzed by RT-qPCR assay after transfected of miR-9-5p mimic and inhibtor.

(B) The sequence of NHE1 wild-type 3′UTR with predicted targeting site containing base complementarity with miR-9-5p and NHE1 mutated 3′UTR.

(C) The fluorescence intensity was greatly decreased after co-expression of miR-9-5p and NHE1 reporter in wild type. NHE1 promoter constructs containing a potential miR-9-5p binding motif.

(D) RIP assays for Ago2 and miR-9-5p binding. Antibodies anti-IgG and anti-Ago2 were used in the RIP assays. qRT-PCR was performed to quantify the binding activity.

(E) Expression levels of IDH1 K224Ac in human CRC tumor and normal tissue specimens, assessed by immunohistochemistry.

Figure 5. *Continued*

(F) Mutation of IDH1 K224R and K224Q resulted in altered protein levels of NHE1 and Ago2 by western blot.

(G) IDH1 K224 deacetylation regulates cellular α-KG levels in cells. In HCT116 stable cells with IDH1 knockout and re-expressing the indicated proteins, the α-KG levels in cells was measured in OD values at different time point.

(H) Expression levels of Ago2 and NHE1 with addition of α-KG in the cell medium.

(I–K) The expression of NHE1 mRNA and protein and the pH value of culture medium altered after adding α-KG to different stable cell lines.

K224R HCT116 cells. Slower xenograft tumor growth was observed in the IDH1 K224R group (Figures 7A, 7B, and 7D) compared to the IDH1 WT or IDH1 K224Q group. These findings imply that IDH1 K224 deacetylation exerts a suppressive effect on CRC growth *in vivo*. Moreover, as shown in Figure 7C, we investigated IDH1 K224 acetylation levels in xenograft tumor tissues. The Ago2 and NHE1 antibodies were used to detect the expression levels of these two proteins in xenograft tumor tissues. The results showed that Ago2 expression was significantly decreased in IDH1 K224Q group tissues compared to other group tissues, while the expression of NHE1 showed the opposite pattern. These results suggest that the downregulation of IDH1 K224 acetylation could lead to Ago2 expression upregulation and NHE1 expression downregulation. A schematic depiction of the proposed interaction mechanism is shown in Figure 7E.

DISCUSSION

The five-year survival rate for metastatic CRC is very low, even when combined with chemotherapy, molecular targeting treatment, and radiotherapy.[26,27] In particular, liver metastasis is a challenge in CRC treatment. However, the molecular mechanisms underlying the progression and liver metastasis of CRC have not been completely elucidated. Protein lysine acetylation, specifically non-histone acetylation modification, is involved in the occurrence and development of various tumors—especially in the invasion and metastasis of CRC.[28–30] In previous studies, we identified a complete atlas of acetylome in CRC and paired liver metastases and demonstrated that SIRT2 suppresses CRC cell progression and liver metastases by regulating IDH1 acetylation and its enzymatic activity.[8,23] In the present study, we present evidence suggesting that the substrate α-KG of IDH1 together with PHD regulates Ago2 expression. Furthermore, we propose that IDH1 regulates the extracellular acidic microenvironment via the α-KG induced miR-9-5p/NHE1 signal pathway.

An acidic microenvironment can promote the occurrence and development of CRC. Active glycolysis produces many acidic products that create an acidic microenvironment with strong toxicity to adjacent normal cells, which is conducive to tumor invasion of adjacent normal tissues. Therefore, the establishment of an acidic microenvironment is an essential process of tumor metastasis.[31] Some studies have reported that acidic medium treatment can significantly enhance the invasion and metastatic ability of CRC cells.[32] In contrast, an acidic microenvironment around tumor cells can also cause tumor cell-cycle arrest, inhibit cell proliferation, and induce apoptosis. Thus, the acidic microenvironment appears to have extensive and complex effects on tumor cells, and inhibition of the acidic microenvironment can effectively interfere with tumor progression.[33] Our results suggest that, within a certain range, the invasive ability of CRC cells increases with a decreasing pH value of the cell culture medium.

α-KG is a potent antineoplastic metabolite which can drive tumor cell differentiation and antagonize malignant progression[34] and in CRC it significantly restricts tumor growth and extend survival through attenuating Wnt signaling.[35] While IDH1 is a key enzyme converting isocitrate to α-KG, which greatly affects the TAC. When TAC is disturbed, pyruvic acid transforms to lactic acid, thereby contributing to an acidic intracellular environment. IDH1 has been mainly studied in other cancers such as glioma[36] and acute myelogenous leukemia.[37] In contrast, the function of IDH1 in CRC remains unclear. Previously, we assessed IDH1 as a PTM and its functions in CRC and revealed the critical role of IDH1 K224 acetylation in the promotion of the α-KG/HIF1α/SRC signaling pathway in the metastasis process of CRC and elucidated the mechanism of IDH1 acetylation regulation in primary CRC tissues and liver metastatic tissues. We analyzed the acetylation features of IDH1 using the CPLM tool and found that acetylation on K224 was significant for IDH1. Also, in the current study, IDH1 K224R led to increasing pH of CRC cell medium, demonstrating that IDH1 acetylation is involved in the regulation of the acidic microenvironment in CRC.

The ion transporters that maintain the abnormal pH gradient of tumor cells include the NHE, vacuolar proton pump (V-ATPase), Na^+-dependent Cl^-/HCO_3^- exchanger (NCBE), etc. Among them, NHE is the most important for balancing and regulating the acidic microenvironment inside and outside cells and has received the most in-depth research. Among the eight NHE subtypes, subtype 1 (NHE1) is the most widely

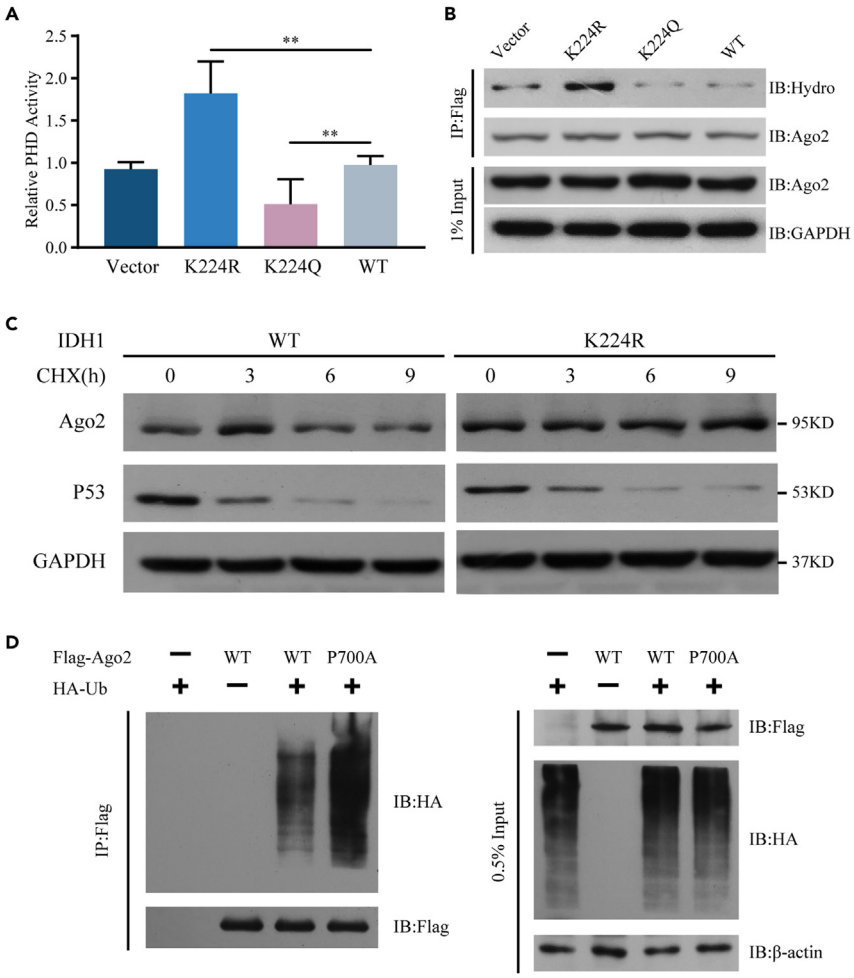

Figure 6. The acetylation of IDH1 changes the stability of Ago2

(A) Mutation of IDH1 K224R and K224Q altered PHD catalytic activity.

(B) Ago2 hydroxylation level was enhanced with mutation of K224R. Flag-Ago2 was overexpressed in different acetylation of IDH1 cells. Ago2 hydroxylation level was determined by western blot.

(C) Mutation of IDH1 K224R can extend the half-life of Ago2. Cycloheximide (CHX) was added to the medium at different time point, and western blot was used to determine the Ago2. P53 was used as a positive reference.

(D) Mutations at the P700 site of Ago2 inhibited its hydroxylation and increased its own ubiquitination degradation.

expressed and plays a key role in the regulation of extracellular pH. The incidence of tumor events is significantly reduced in cells lacking NHE1 expression.[38] Downregulation of NHE1 expression has been shown to significantly inhibit the invasion and metastasis of various tumor cells, such as glioma,[39] pancreatic cancer,[40] breast cancer,[41] gastric cancer,[42] and CRC.[13] Our results suggest that IDH1 K224 acetylation may downregulate the pH of the extracellular microenvironment via NHE1. In the TCGA database, NHE1 adversely affects patient survival in a variety of cancers, with the exception of colorectal cancer. We speculate that this may be related to the presence of a large number of NHE1 in the healthy human intestine due to physiological factors,[43] which masks its role in tumor promotion.

The generation of mature miRNA is completed by multiple splicing steps involving the actions of a variety of enzymes: Firstly, primary miRNA (pri-miRNA) is generated by gene transcription, which is then processed into precursor miRNA (pre-miRNA) with Drosha nuclease. The pre-miRNA is transferred to the cytoplasm through transporters and generated into mature miRNA by the Dicer enzyme.[44] Mature miRNA and RISC form a complex to regulate the mRNA expression of downstream genes. Ago2 is an essential part of the RISC complex that regulates miRNA expression or production.[15] Although Dicer is not necessary for the generation of certain miRNAs, Ago2 is required.[16] Ago2 stability is regulated by its own PTM, particularly

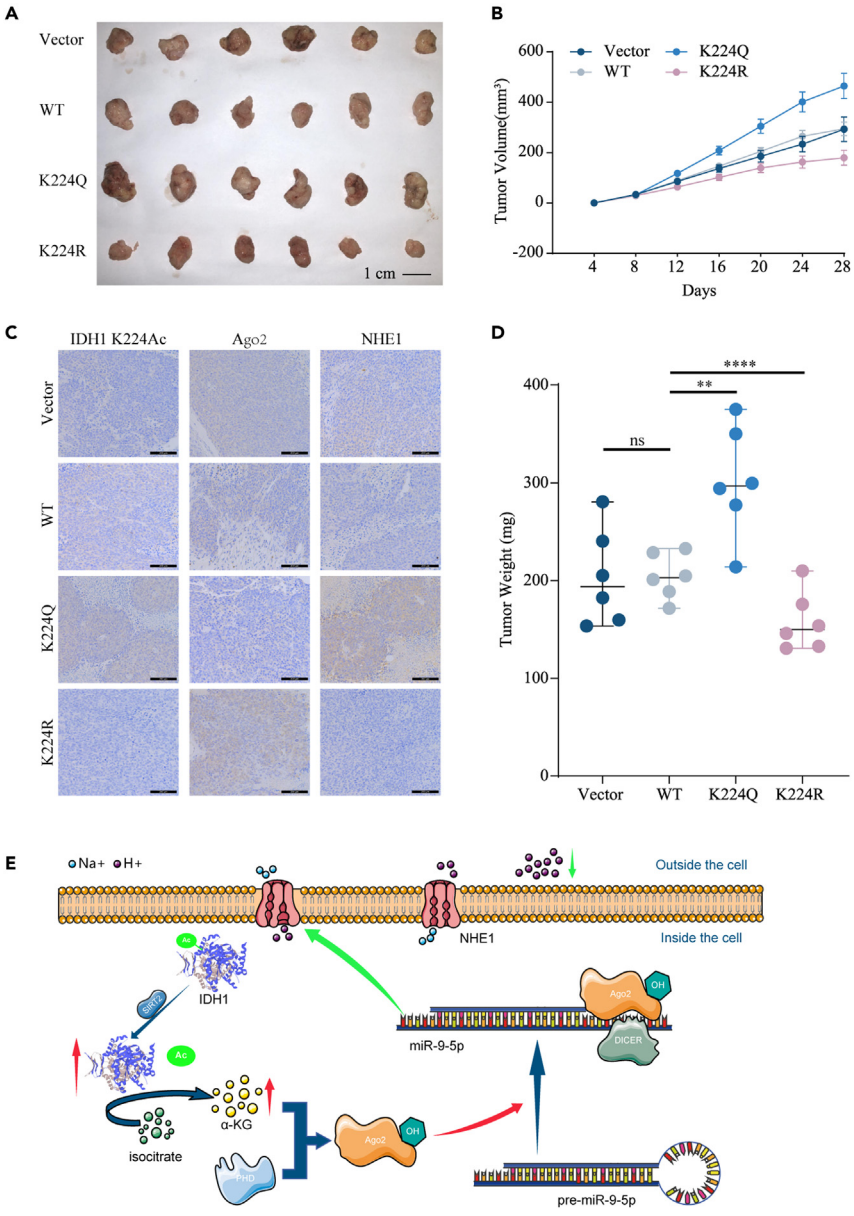

Figure 7. IDH1 K224 deacetylation impairs CRC growth *in vivo*

(A) Pictures of the tumors after nude mice being sacrificed were shown in four subgroups.

(B) Tumor volumes of each group during the tumor growth process.

(C) Immunohistochemical analysis of IDH1 K224A、Ago2、NHE1 protein in representative xenograft model.

(D) Tumor weight measured from the xenograft model.

(E) A working model illustrating regulation of this study.

hydroxylation. Prolyl-4-hydroxylase is reported to interact with Ago2 and hydroxylates Ago2 at proline 700, and mutation of proline 700 to alanine results in destabilization of Ago2.[14] Wu et al. demonstrated that hydroxylation of Ago2 increases the level of miRNAs and increases the endonuclease activity of Ago2.[15] As the mutation of proline to alanine at position 700 can also cause instability of Ago2, regulation of proline at position 700 and hydroxylation of this residue influence its stability. This finding indicates that hydroxylation as a PTM is important for the stability of Ago2 and effective RNA interference.[14] The hydroxylation of Ago2 is required for its interaction with heat shock protein 90, and this interaction is necessary for the assembly of miRNA into the RISC complex and its transfer to stress particles. Hydroxylation of Ago2 has been shown to enhance the expression of miRNA and the endonuclease activity of Ago2.[15]

To further explore the mechanism by which IDH1 K224 acetylation regulates NHE1 through Ago2/miRNA pathway, we used the microRNA microarray to evaluate miRNAs expression after hypoacetylation of IDH1 K224, and found that IDH1 acetylation affected the expression of Ago2 through the PHD enzyme and then regulated miR-9-5p expression. Hydroxylation is an important PTM that plays important biological roles. PHD hydroxylation of Ago2 is essential for its functional folding and stability, and further impairs downstream targets such as miRNA regulation. Using microarray detection, we identified differential miRNAs in colon cancer cells with different acetylation status of IDH1. Next, using bioinformatics methods, we confirmed that these miRNAs were associated with various tumors. Focusing on miR-9-5p, which showed the most obvious changes, we determined that its target genes were related to oxygen levels via KEGG pathway enrichment. Overall, these findings are consistent with our hypothesis. The change in IDH 1 activity leads to disorders of glucose metabolism, which makes cells more likely to undergo glycolysis and produce acidic substances. Subsequent exploration in this study revealed that miR-9-5p is associated with various types of T cells, which is likely due to changes in the acidic microenvironment outside of tumor cells. The change in pH of the microenvironment may result in changes in the proliferation of immune cells diffused there. However, further experiments are needed to verify these hypotheses.

In addition, we demonstrated that NHE1 3′UTR is targeted by miR-9-5p. Recent reports have shown that miR-9-5p mediates cell invasion, metastasis, proliferation, and apoptosis by targeting different mRNAs such as TM4SF1 and UHRF1.[45–47] Further studies have shown that the promotion of CRC caused by acetylation of IDH1 can be counteracted by exogenous ketoglutarate and also alter the pH value of culture medium. Interestingly, we also found that changes in NHE1 expression caused by changes in IDH1 acetylation levels may also be related to lymphocyte infiltration in the tumor immune microenvironment, which of course needs further experimental verification.

Taken together, the results of this study have demonstrated an important mechanism of IDH1 regulation of the extracellular acidic microenvironment. NHE1, as a key acid-base transporter, can be regulated by IDH1 K224 acetylation through the miR-9-5p/Ago2 complex in CRC. α-KG, as a catalyst of IDH1, may stabilize Ago2 protein expression by enhancing hydroxylation and reducing ubiquitination. These findings suggest a potential strategy for CRC therapy by targeting IDH1 K224 or the Ago2/miR-9-5p/NHE1 axis.

STAR★METHODS

Detailed methods are provided in the online version of this paper and include the following:

- KEY RESOURCES TABLE
- RESOURCE AVAILABILITY
  - Lead contact
  - Materials availability
  - Data and code availability
- EXPERIMENTAL MODELS AND SUBJECT DETAILS
  - Patients and CRC tissue specimenss
  - Cell culture
  - Animal models
- METHOD DETAILS
  - MicroRNAs microarray analysis
  - Bioinformatics analysis of miRNA
  - miRNA target prediction
  - Dual-luciferase reporter assay
  - RNA immunoprecipitation (RIP) assay
  - siRNA synthesis and cell transfection
  - pH measurement
  - Protein extraction and western blot analysis
  - qRT-PCR analysis
  - Co-immunoprecipitation
  - Protein stability and hydroxylation experiment
  - Cell proliferation assays
  - Wound healing and invasion assays
  - Plasmid mutation
- QUANTIFICATION AND STATISTICAL ANALYSIS

SUPPLEMENTAL INFORMATION

Supplemental information can be found online at https://doi.org/10.1016/j.isci.2023.107206.

ACKNOWLEDGMENTS

This work was supported by the National Natural Science Foundation of China (Grant No. 82272841 and 81972240).

AUTHOR CONTRIBUTIONS

B.W. and L.Z. contributed to the conception and design of the study. L.Z. extracted the data and C.J.Y. analyzed the data. B.W. drafted the manuscript. Y.L.L. and S.W. contributed to a critical revision of the manuscript. Z.L.S. completed critical review and funding support. Y.J.Y collect and interpret the data, J.Y.L performed overall supervision, Z.L.S. revised the manuscript. All authors have read and approved the final version of the manuscript.

DECLARATION OF INTERESTS

The authors declare that they have no known competing financial interests or personal relationships that could have appeared to influence the work reported in this paper.

Received: October 25, 2022
Revised: April 10, 2023
Accepted: June 21, 2023
Published: June 25, 2023

REFERENCES

1. Chen, W., Zheng, R., Baade, P.D., Zhang, S., Zeng, H., Bray, F., Jemal, A., Yu, X.Q., and He, J. (2016). Cancer statistics in China, 2015. CA. Cancer J. Clin. *66*, 115–132. https://doi.org/10.3322/caac.21338.

2. Fakih, M.G. (2015). Metastatic colorectal cancer: current state and future directions. J. Clin. Oncol. *33*, 1809–1824. https://doi.org/10.1200/JCO.2014.59.7633.

3. Warburg, O., Wind, F., and Negelein, E. (1927). THE METABOLISM OF TUMORS IN THE BODY. J. Gen. Physiol. *8*, 519–530.

4. Boedtkjer, E., and Pedersen, S.F. (2020). The Acidic Tumor Microenvironment as a Driver of Cancer. Annu. Rev. Physiol. *82*, 103–126. https://doi.org/10.1146/annurev-physiol-021119-034627.

5. Vaupel, P., and Multhoff, G. (2021). Revisiting the Warburg effect: historical dogma versus current understanding. J. Physiol. *599*, 1745–1757. https://doi.org/10.1113/JP278810.

6. De Milito, A., Iessi, E., Logozzi, M., Lozupone, F., Spada, M., Marino, M.L., Federici, C., Perdicchio, M., Matarrese, P., Lugini, L., et al. (2007). Proton pump inhibitors induce apoptosis of human B-cell tumors through a caspase-independent mechanism involving reactive oxygen species. Cancer Res. *67*, 5408–5417.

7. Kislin, K.L., McDonough, W.S., Eschbacher, J.M., Armstrong, B.A., and Berens, M.E. (2009). NHERF-1: modulator of glioblastoma cell migration and invasion. Neoplasia *11*, 377–387.

8. Shen, Z., Wang, B., Luo, J., Jiang, K., Zhang, H., Mustonen, H., Puolakkainen, P., Zhu, J., Ye, Y., and Wang, S. (2016). Global-scale profiling of differential expressed lysine acetylated proteins in colorectal cancer tumors and paired liver metastases. J. Proteomics *142*, 24–32. https://doi.org/10.1016/j.jprot.2016.05.002.

9. Liu, J., Peng, Y., Shi, L., Wan, L., Inuzuka, H., Long, J., Guo, J., Zhang, J., Yuan, M., Zhang, S., et al. (2021). Skp2 dictates cell cycle-dependent metabolic oscillation between glycolysis and TCA cycle. Cell Res. *31*, 80–93. https://doi.org/10.1038/s41422-020-0372-z.

10. Metallo, C.M., Gameiro, P.A., Bell, E.L., Mattaini, K.R., Yang, J., Hiller, K., Jewell, C.M., Johnson, Z.R., Irvine, D.J., Guarente, L., et al. (2011). Reductive glutamine metabolism by IDH1 mediates lipogenesis under hypoxia. Nature *481*, 380–384. https://doi.org/10.1038/nature10602.

11. Toft, N.J., Axelsen, T.V., Pedersen, H.L., Mele, M., Burton, M., Balling, E., Johansen, T., Thomassen, M., Christiansen, P.M., and Boedtkjer, E. (2021). Acid-base transporters and pH dynamics in human breast carcinomas predict proliferative activity, metastasis, and survival. Elife *10*, e68447. https://doi.org/10.7554/eLife.68447.

12. Iorio, J., Duranti, C., Lottini, T., Lastraioli, E., Bagni, G., Becchetti, A., and Arcangeli, A. (2020). K11.1 Potassium Channel and the Na/H Antiporter NHE1 Modulate Adhesion-Dependent Intracellular pH in Colorectal Cancer Cells. Front. Pharmacol. *11*, 848. https://doi.org/10.3389/fphar.2020.00848.

13. Rebillard, A., Tekpli, X., Meurette, O., Sergent, O., LeMoigne-Muller, G., Vernhet, L., Gorria, M., Chevanne, M., Christmann, M., Kaina, B., et al. (2007). Cisplatin-induced apoptosis involves membrane fluidification via inhibition of NHE1 in human colon cancer cells. Cancer Res. *67*, 7865–7874.

14. Qi, H.H., Ongusaha, P.P., Myllyharju, J., Cheng, D., Pakkanen, O., Shi, Y., Lee, S.W., Peng, J., and Shi, Y. (2008). Prolyl 4-hydroxylation regulates Argonaute 2 stability. Nature *455*, 421–424. https://doi.org/10.1038/nature07186.

15. Wu, C., So, J., Davis-Dusenbery, B.N., Qi, H.H., Bloch, D.B., Shi, Y., Lagna, G., and Hata, A. (2011). Hypoxia potentiates microRNA-mediated gene silencing through posttranslational modification of Argonaute2. Mol. Cell Biol. *31*, 4760–4774. https://doi.org/10.1128/MCB.05776-11.

16. Cheloufi, S., Dos Santos, C.O., Chong, M.M.W., and Hannon, G.J. (2010). A dicer-independent miRNA biogenesis pathway that requires Ago catalysis. Nature *465*, 584–589. https://doi.org/10.1038/nature09092.

17. Chang, J., Davis-Dusenbery, B.N., Kashima, R., Jiang, X., Marathe, N., Sessa, R., Louie, J., Gu, W., Lagna, G., and Hata, A. (2013). Acetylation of p53 stimulates miRNA processing and determines cell survival following genotoxic stress. EMBO J. *32*, 3192–3205. https://doi.org/10.1038/emboj.2013.242.

18. Kim, J.O., Kwon, E.J., Song, D.W., Lee, J.S., and Kim, D.H. (2016). miR-185 inhibits endoplasmic reticulum stress-induced

apoptosis by targeting Na+/H+ exchanger-1 in the heart. BMB Rep. *49*, 208–213.

19. Koumangoye, R.B., Andl, T., Taubenslag, K.J., Zilberman, S.T., Taylor, C.J., Loomans, H.A., and Andl, C.D. (2015). SOX4 interacts with EZH2 and HDAC3 to suppress microRNA-31 in invasive esophageal cancer cells. Mol. Cancer *14*, 24. https://doi.org/10.1186/s12943-014-0284-y.

20. Lee, J.J., Drakaki, A., Iliopoulos, D., and Struhl, K. (2012). MiR-27b targets PPARγ to inhibit growth, tumor progression and the inflammatory response in neuroblastoma cells. Oncogene *31*, 3818–3825. https://doi.org/10.1038/onc.2011.543.

21. Lee, S.-W., Yang, J., Kim, S.-Y., Jeong, H.-K., Lee, J., Kim, W.J., Lee, E.J., and Kim, H.-S. (2015). MicroRNA-26a induced by hypoxia targets HDAC6 in myogenic differentiation of embryonic stem cells. Nucleic Acids Res. *43*, 2057–2073. https://doi.org/10.1093/nar/gkv088.

22. Mullany, L.E., and Slattery, M.L. (2019). The functional role of miRNAs in colorectal cancer: insights from a large population-based study. Cancer Biol. Med. *16*, 211–219. https://doi.org/10.20892/j.issn.2095-3941.2018.0514.

23. Wang, B., Ye, Y., Yang, X., Liu, B., Wang, Z., Chen, S., Jiang, K., Zhang, W., Jiang, H., Mustonen, H., et al. (2020). SIRT2-dependent IDH1 deacetylation inhibits colorectal cancer and liver metastases. EMBO Rep. *21*, e48183. https://doi.org/10.15252/embr.201948183.

24. Chen, J., Lai, F., and Niswander, L. (2012). The ubiquitin ligase mLin41 temporally promotes neural progenitor cell maintenance through FGF signaling. Genes Dev. *26*, 803–815. https://doi.org/10.1101/gad.187641.112.

25. Johnston, M., Geoffroy, M.-C., Sobala, A., Hay, R., and Hutvagner, G. (2010). HSP90 protein stabilizes unloaded argonaute complexes and microscopic P-bodies in human cells. Mol. Biol. Cell *21*, 1462–1469. https://doi.org/10.1091/mbc.E09-10-0885.

26. Chua, T.C., Saxena, A., Liauw, W., Chu, F., and Morris, D.L. (2012). Hepatectomy and resection of concomitant extrahepatic disease for colorectal liver metastases–a systematic review. Eur. J. Cancer *48*, 1757–1765. https://doi.org/10.1016/j.ejca.2011.10.034.

27. Hwang, M., Jayakrishnan, T.T., Green, D.E., George, B., Thomas, J.P., Groeschl, R.T., Erickson, B., Pappas, S.G., Gamblin, T.C., and Turaga, K.K. (2014). Systematic review of outcomes of patients undergoing resection for colorectal liver metastases in the setting of extra hepatic disease. Eur. J. Cancer *50*, 1747–1757. https://doi.org/10.1016/j.ejca.2014.03.277.

28. Jiang, H., Wu, L., Chen, J., Mishra, M., Chawsheen, H.A., Zhu, H., and Wei, Q. (2015). Sulfiredoxin Promotes Colorectal Cancer Cell Invasion and Metastasis through a Novel Mechanism of Enhancing EGFR Signaling. Mol. Cancer Res. *13*, 1554–1566. https://doi.org/10.1158/1541-7786.MCR-15-0240.

29. Liu, X., Tan, Y., Zhang, C., Zhang, Y., Zhang, L., Ren, P., Deng, H., Luo, J., Ke, Y., and Du, X. (2016). NAT10 regulates p53 activation through acetylating p53 at K120 and ubiquitinating Mdm2. EMBO Rep. *17*, 349–366. https://doi.org/10.15252/embr.201540505.

30. Zhou, J., Zhan, S., Tan, W., Cheng, R., Gong, H., and Zhu, Q. (2014). P300 binds to and acetylates MTA2 to promote colorectal cancer cells growth. Biochem. Biophys. Res. Commun. *444*, 387–390. https://doi.org/10.1016/j.bbrc.2014.01.062.

31. Gillies, R.J., Robey, I., and Gatenby, R.A. (2008). Causes and consequences of increased glucose metabolism of cancers. J. Nucl. Med. *49* (*Suppl 2*), 24S–42S. https://doi.org/10.2967/jnumed.107.047258.

32. Zhao, M., Liu, Q., Gong, Y., Xu, X., Zhang, C., Liu, X., Zhang, C., Guo, H., Zhang, X., Gong, Y., and Shao, C. (2016). GSH-dependent antioxidant defense contributes to the acclimation of colon cancer cells to acidic microenvironment. Cell Cycle *15*, 1125–1133. https://doi.org/10.1080/15384101.2016.1158374.

33. Martinez-Outschoorn, U.E., Peiris-Pagés, M., Pestell, R.G., Sotgia, F., and Lisanti, M.P. (2017). Cancer metabolism: a therapeutic perspective. Nat. Rev. Clin. Oncol. *14*, 11–31. https://doi.org/10.1038/nrclinonc.2016.60.

34. Morris, J.P., Yashinskie, J.J., Koche, R., Chandwani, R., Tian, S., Chen, C.-C., Baslan, T., Marinkovic, Z.S., Sánchez-Rivera, F.J., Leach, S.D., et al. (2019). α-Ketoglutarate links p53 to cell fate during tumour suppression. Nature *573*, 595–599. https://doi.org/10.1038/s41586-019-1577-5.

35. Tran, T.Q., Hanse, E.A., Habowski, A.N., Li, H., Ishak Gabra, M.B., Yang, Y., Lowman, X.H., Ooi, A.M., Liao, S.Y., Edwards, R.A., et al. (2020). α-Ketoglutarate attenuates Wnt signaling and drives differentiation in colorectal cancer. Nat. Cancer *1*, 345–358. https://doi.org/10.1038/s43018-020-0035-5.

36. Bralten, L.B.C., Kloosterhof, N.K., Balvers, R., Sacchetti, A., Lapre, L., Lamfers, M., Leenstra, S., de Jonge, H., Kros, J.M., Jansen, E.E.W., et al. (2011). IDH1 R132H decreases proliferation of glioma cell lines in vitro and in vivo. Ann. Neurol. *69*, 455–463. https://doi.org/10.1002/ana.22390.

37. Losman, J.-A., Looper, R.E., Koivunen, P., Lee, S., Schneider, R.K., McMahon, C., Cowley, G.S., Root, D.E., Ebert, B.L., and Kaelin, W.G. (2013). (R)-2-hydroxyglutarate is sufficient to promote leukemogenesis and its effects are reversible. Science (New York, N.Y.) *339*, 1621–1625. https://doi.org/10.1126/science.1231677.

38. Harguindey, S., Orive, G., Luis Pedraz, J., Paradiso, A., and Reshkin, S.J. (2005). The role of pH dynamics and the Na+/H+ antiporter in the etiopathogenesis and treatment of cancer. Two faces of the same coin–one single nature. Biochim. Biophys. Acta *1756*, 1–24.

39. Cong, D., Zhu, W., Shi, Y., Pointer, K.B., Clark, P.A., Shen, H., Kuo, J.S., Hu, S., and Sun, D. (2014). Upregulation of NHE1 protein expression enables glioblastoma cells to escape TMZ-mediated toxicity via increased H^+ extrusion, cell migration and survival. Carcinogenesis *35*, 2014–2024. https://doi.org/10.1093/carcin/bgu089.

40. Cardone, R.A., Greco, M.R., Zeeberg, K., Zaccagnino, A., Saccomano, M., Bellizzi, A., Bruns, P., Menga, M., Pilarsky, C., Schwab, A., et al. (2015). A novel NHE1-centered signaling cassette drives epidermal growth factor receptor-dependent pancreatic tumor metastasis and is a target for combination therapy. Neoplasia *17*, 155–166. https://doi.org/10.1016/j.neo.2014.12.003.

41. Amith, S.R., and Fliegel, L. (2013). Regulation of the Na+/H+ Exchanger (NHE1) in Breast Cancer Metastasis. Cancer Res. *73*, 1259–1264. https://doi.org/10.1158/0008-5472.CAN-12-4031.

42. Xia, J., Huang, N., Huang, H., Sun, L., Dong, S., Su, J., Zhang, J., Wang, L., Lin, L., Shi, M., et al. (2016). Voltage-gated sodium channel Nav 1.7 promotes gastric cancer progression through MACC1-mediated upregulation of NHE1. Int. J. Cancer *139*, 2553–2569. https://doi.org/10.1002/ijc.30381.

43. Nikolovska, K., Seidler, U.E., and Stock, C. (2022). The Role of Plasma Membrane Sodium/Hydrogen Exchangers in Gastrointestinal Functions: Proliferation and Differentiation, Fluid/Electrolyte Transport and Barrier Integrity. Front. Physiol. *13*, 899286. https://doi.org/10.3389/fphys.2022.899286.

44. Ambros, V. (2004). The functions of animal microRNAs. Nature *431*, 350–355.

45. Park, Y.R., Lee, S.T., Kim, S.L., Liu, Y.C., Lee, M.R., Shin, J.H., Seo, S.Y., Kim, S.H., Kim, I.H., Lee, S.O., and Kim, S.W. (2016). MicroRNA-9 suppresses cell migration and invasion through downregulation of TM4SF1 in colorectal cancer. Int. J. Oncol. *48*, 2135–2143. https://doi.org/10.3892/ijo.2016.3430.

46. Zhu, L., Chen, H., Zhou, D., Li, D., Bai, R., Zheng, S., and Ge, W. (2012). MicroRNA-9 up-regulation is involved in colorectal cancer metastasis via promoting cell motility. Med. Oncol. *29*, 1037–1043. https://doi.org/10.1007/s12032-011-9975-z.

47. Zhu, M., Xu, Y., Ge, M., Gui, Z., and Yan, F. (2015). Regulation of UHRF1 by microRNA-9 modulates colorectal cancer cell proliferation and apoptosis. Cancer Sci. *106*, 833–839. https://doi.org/10.1111/cas.12689.

STAR★METHODS

KEY RESOURCES TABLE

REAGENT or RESOURCE	SOURCE	IDENTIFIER
Antibodies		
Rabbit Polyclonal Anti-IDH1	Abcam	Cat # ab172964
Rabbit Polyclonal Anti-Ago2	Abcam	Cat # ab186733
Rabbit Polyclonal Anti-NHE1	Abcam	Cat # ab67314
Anti-IDH1 K224Ac antibody	PTM Biolabs Inc.	N/A
Hydroxyproline Antibody	Cell Signaling Technology	Cat # 73812
Rabbit Polyclonal Anti-GAPDH	Cell Signaling Technology	Cat # ab172964
Bacterial and virus strains		
si-NC (5′ to 3′): ACGUGACACGUUCGGAGAATT	GenePharma	N/A
si-NHE1 (5′ to 3′): AGAUAGUGGGGAUCACAUGGA	GenePharma	N/A
Biological samples		
CRC tissue microarray	Peking University People's Hospital	N/A
Chemicals, peptides, and recombinant proteins		
TRIzol	Invitrogen	Cat # 15596026
RIPA Lysis Buffer	Applygen	Cat #C1053-100
RNase R	Lucigen	Cat # RNR07250
Lipofectamine 3000	Invitrogen	Cat #L3000001
Matrigel Matrix	Corning	Cat # 356234
Critical commercial assays		
1st Strand cDNA Synthesis SuperMix for qPCR	Yeasen	Cat # 11141ES10
qPCR SYBR Green Master Mix	Yeasen	Cat # 11199ES03
KOD Plus Mutagenesis Kit	TOYOBO	Cat # SMK-101
Cell Counting Kit-8 (CCK8)	Sigma	Cat # 96992
BCA Protein Assay Kit	Kangwei Century Co.	Cat # CW0014
Pierce ECL Western	Thermo Fisher	Cat # 32106
Dual-Luciferase® Reporter (DLR™) Assay System	Promega	Cat #E1910
Deposited data		
miRNA microarray data	This paper	N/A
Experimental models: Cell lines		
SW480	American Type Culture Collection	Cat # CCL-228
HCT116	American Type Culture Collection	Cat # CCL-247
Experimental models: Organisms/strains		
BALB/c nude mice	Vital River Laboratories	N/A
Oligonucleotides		
NHE1 forward: 5′-GGGGAGGGACTGCTGAC-3′	This paper	N/A
NHE1 reverse: 5′-AGGACAGGTTGGGTGGTG-3′	This paper	N/A
NBC1 forward: 5′-CACAATCTCTAGGGTAAGCCA-3′	This paper	N/A
NBC1 reverse: 5′-GTCTCTTCTCCCTCAATCTCC-3′	This paper	N/A
ATP4B forward: 5′-CAGGAGGACAGCATCAACT-3′	This paper	N/A

(*Continued on next page*)

Continued

REAGENT or RESOURCE	SOURCE	IDENTIFIER
ATP4B reverse: 5′-CGTGAACTTGCAGGAGAAC-3′	This paper	N/A
Ago2 forward: 5′-CAGTGCGTGCAGATGAAG-3′	This paper	N/A
Ago2 reverse: 5′-GGCAGCAGGATGTTGTTC-3′	This paper	N/A
Software and algorithms		
ImageJ	NIH	N/A
GraphPad Prism 8	GraphPad	N/A
The R Project for Statistical Computing	Datagurn	N/A
Other		
Fetal bovine serum	Gibco	Cat # 16000-044
Dulbecco's Modified Eagle Medium (DMEM)	Gibco	Cat # 12491015
Penicillin	Sigma-Aldrich	Cat # 52-67-5
Streptomycin	Sigma-Aldrich	Cat # SBR00068

RESOURCE AVAILABILITY

Lead contact

Further information and requests for resources and reagents should be directed to and will be fulfilled by the lead contact, Zhanlong Shen (shenzhanlong@pkuph.edu.cn)

Materials availability

The study did not generate new unique reagents.

Data and code availability

- The Cancer Genome Atlas (TCGA) (https://cancergenome.nih.gov/) databases were employed for retrieving all original data.
- The Human Protein Atlas (HPA) (https://www.proteinatlas.org/) was then utilized for confirming the degree of IDH1 immunohistochemical staining in CRC tissues.
- R 3.1.2 was employed for integrating the original information and validating the outcomes of the website database analysis. Entire utilized internet web tools were presented below, and employing the "ggplot2" R package, the box diagrams were drawn.
- This paper does not report original code.
- Any additional information required to reanalyze the data reported in this paper is available from the lead contact upon request.

EXPERIMENTAL MODELS AND SUBJECT DETAILS

Patients and CRC tissue specimenss

Tissue microarrays were obtained from the surgical oncology laboratory of Peking University People's Hospital. Written informed consent was provided by all patients before sample collection. The local Research Ethics Committee of Peking University People's Hospital approved this study.

Cell culture

The human CRC cell lines SW480 and HCT116 were purchased from the American Type Culture Collection (ATCC). All cells were cultured at 37°C in a humidified environment containing 5% CO2 in Dulbecco's modified eagle medium (DMEM) and supplemented with 10% fetal bovine serum (FBS, Gibco), 100 U/ml penicillin (Sigma-Aldrich), and 100 μg/mL streptomycin (Sigma-Aldrich). All cell lines were tested for mycoplasma contamination and authenticated by short tandem repeat profiling.

Animal models

All experimental procedures were approved by the Animal Care Committee of the Peking University People's Hospital. BALB/c nude mice (6 weeks old, purchased from Beijing Vital River Laboratories, China) were housed in an environment with temperature of 22 ± 1°C, relative humidity of 50 ± 1%, and a light/dark cycle of 12/12 h. All animal studies (including the mice euthanasia procedure) were done in compliance with the regulations and guidelines of Peking University People's Hospital institutional animal care and conducted according to the AAALAC and the IACUC guidelines.

METHOD DETAILS

MicroRNAs microarray analysis

For miRNA microarray analysis, total RNAs were extracted from the CRC cells transfected with WT IDH1 plasmid and IDH1 K224R plasmid. Sample preparation and microarray hybridization were performed according to Arraystar standard protocols. The Agilent feature extraction program was used to examine the acquired array images.

Bioinformatics analysis of miRNA

The TAM2.0 website (http://www.lirmed.com/tam2/), which is a powerful tool for miRNA analysis, was used to further explore the differential miRNAs detected by our microarray. To use this tool, we entered the comparison program and copy and pasted the list of upregulated and downregulated miRNAs into "Step1" and "Step2", respectively, with the other parameters unchanged. We then submitted the request by clicking the "Run" button to obtain a function heat map and bar graph of the upregulated and downregulated miRNAs. To analyze the immune cell correlations of miRNAs in CRC with tumor tissue infiltration, we used R version 4.1.2. The GSVA package was used to analyze the miRNAseq data of level 3 BCGSC miRNA profiling in TCGA's COADREAD project. The miRNAseq data in the RPM (Reads per Million mapped reads) format was log2 transformed. The markers of the 24 immune cells used for analysis were obtained from an article published in Immunity. For the target gene function enrichment analysis of miR-9-5p, we used the CancerMIRNome database (http://bioinfo.jialab-ucr.org/CancerMIRNome/).

miRNA target prediction

miRNA sequences and family information were obtained from the TargetScan 7.2 website (http://www.targetscan.org/). To predict microRNAs regulating NHE1 (gene name SLC9A1) in humans, we entered the human gene symbol "SLC9A1" in the website search bar. The predicted results comprised 865 microRNA including miR-9-5p. The miR-9-5p target was also identified by TargetScan 7.2. The predicted target sites of NHE1 on 3'UTR were obtained from the TargetScan website.

Dual-luciferase reporter assay

HCT116 cells were seeded at a density of 2 × 105 cells per six-well dish. Wild type (WT) or mutant NHE1 3'UTR containing the miR-9-5p binding sequences was synthesized and cloned into the pGL3-Basic Vector (Promega, Beijing, China). The HCT116 cells were co-transfected with constructed vector and miR-9-5p mimics or miRNA NC using Lipofectamine2000. Next, 48 h after transfection, luciferase activity was assessed using the Dual-Luciferase reporter assay kit (Promega, Beijing, China) and normalized for analysis.

RNA immunoprecipitation (RIP) assay

The RIP assay was performed using a RIP kit (Millipore, Billerica, MA, USA). 1 × 107 HCT116 cells were lysed with lysis buffer and magnetic beads (Thermo Fisher, USA) were conjugated to the anti-Ago2 antibody or IgG antibody. Immunoglobulin G was used as a negative control. After digestion with protease K to remove the protein components, the RNA was extracted using TRIzol (Invitrogen, USA). The RNAs were heated at 92°C for 2 min (to remove the secondary structure) and incubated with Ago2 or IgG in RIP buffer (150 mM KCl, 25 mM Tris pH 7.4, 0.5 mM DTT, 0.5% NP40, 1 mM PMSF) and protease inhibitor (Roche Complete Protease Inhibitor Cocktail Tablets) for 3 h at 4°C. The qRT-PCR assay was then used to measure the expression of miR-9-5p as described above.

siRNA synthesis and cell transfection

Two human siRNA sequences were designed against NHE1 and synthesized by Shanghai GenePharma Co., Ltd. (Shanghai, China). The siRNAs were transfected into cells using Lipofectamine 3000 (Thermo Fisher Scientific) for 48 h and then incubated in DMEM with 10% FBS for 48 h.

The cDNA of IDH1 and Ago2 was amplified and cloned into the pcDNA3.1 vector. The IDH1-mutant constructs were generated using a KOD Plus Mutagenesis Kit (TOYOBO). All expression constructs were verified by Sanger sequencing.

pH measurement

The cell suspension in serum-free culture medium was collected into a centrifuge tube and centrifuged at 10,000 rpm for 10 min. The extracellular pH of the cells was measured by monitoring culture medium pH changes using a pH microelectrode (SI Analytics, Mainz, Germany). We report the average pH $\pm$ standard deviation (SD) measured for all samples.

Protein extraction and western blot analysis

Total protein was extracted with lysis buffer. The protein concentration was determined by the BCA method (Kangwei Century Co., Ltd., Beijing, China). Lysates were denatured with sodium dodecyl sulfate (SDS) sample loading buffer at 95°C for 5 min, separated on 8%–12% polyacrylamide gel, and then transferred to nitrocellulose blotting (NC) membranes (Millipore, Massachusetts, USA). The membranes were blocked with 5% non-fat milk powder in TBST buffer for 45 min at room temperature, incubated overnight at 4°C with primary antibodies, and then incubated with conjugated secondary antibody for 90 min at room temperature. The band signals were visualized using enhanced chemiluminescence (ECL; Pierce, Rockford, IL) and subsequently exposed to a ChemiDocTM XRSC System (Bio-Rad, California, USA).

qRT-PCR analysis

Total RNA was extracted using TRIzol reagent (Invitrogen, United States) according to the manufacturer's instructions. Subsequently, 1 μg of total RNA was converted to cDNA using the 1st Strand cDNA Synthesis Super Mix for qPCR Kit (Yeasen, China). Quantitation of NHE1, NBC1, ATP4B, Ago2 mRNA, and miR-9-5p was performed by real-time fluorescence detection. PCR was performed using qPCR SYBR Green Master Mix (Low Rox Plus) Kit (Yeasen, China). Real-time detection of emission intensity of SYBR green bound to double-stranded DNA was performed using the ABI PRISM 7500 Sequence Detection System (Applied Biosystems). GAPDH PCR products were amplified from the same RNA samples and served as an internal control.

Co-immunoprecipitation

Harvested cells were lysed in BC100 buffer (20 mmol/L Tris-HCl (pH 7.9), 100 mmol/L NaCl, 0.2% NP-40, and 20% glycerol) containing protease inhibitor cocktail (Selleck), 1 mmol/L dithiothreitol, and 1 mmol/L phenylmethyl sulfonyl fluoride. Whole lysates were treated with DNase I for 1 h and then incubated with 2 μg of mouse anti-Flag or rabbit anti-HA. Briefly, bound proteins were eluted with loading buffer and the elution was analyzed by Western blot analysis with the Ago2 or hydroxyl antibody.

Protein stability and hydroxylation experiment

Cycloheximide (CHX), which is a protein synthesis inhibitor, acts on the large subunit of the eukaryotic ribosome, inhibits transpeptidase, blocks peptide chain extension, and further inhibits protein synthesis. Approximately 30 h after transfection, CHX (HY12320; MedChemExpress) was added to the CRC cell culture medium at a concentration of 100 μg/mL and the total protein was extracted for Western blot analysis. To eliminate any effects due to protein ubiquitination degradation, we used MG132, a proteasome inhibitor, to inhibit protein degradation in a proteasome dependent manner. Approximately 48 h after transfection, 5 μM MG132 (HY12359; MedChemExpress) was added to the CRC cell culture medium and the same amount of dimethyl sulfoxide (DMSO) was added to the control group. Eleven h after this treatment, the total protein was extracted for Western blot analysis. We used the immunoprecipitation (IP) method to enrich the protein and the hydroxylation antibody to detect alterations in the hydroxylation modification level of Ago2 in the different cell lines.

Cell proliferation assays

To measure cell proliferation, we seeded 1500 cells per well in a 96-well plate. After 24 hours, we measured cell viability using the CCK8 reagent, which we considered day 0. We continued to analyze cell viability every 24 hours and normalized the absorbance to that measured on day 0. We graphed the fold change in cell growth from day 0 to day 4.

Wound healing and invasion assays

HCT116 and SW480 cells transfected with si-NHE1 and si-NC were seeded in six-well plates until about 90% cell confluence was reached. Subsequently, a vertical wound was scratched in the middle of the wells using a 200 μL microtip. Images were captured at 0, 18, and 36 h to assess wound closure. The cell invasion assay was performed in a Transwell chamber with 8 μm pores (Product #3422, Corning Costar Corp., United States). Cells (8 × 104) were prepared in the same way as above in serum-free media and seeded into the upper chamber and media containing 30% FBS was placed in the lower chamber as a chemoattractant for the invasion assays (with Matrigel, Sigma). After 48 h of incubation, the membranes were fixed with 4% paraformaldehyde and stained with 0.1% crystal violet for microscopic analysis.

Plasmid mutation

Lysine (K) is positively charged, and acetylation neutralizes the charge. After point mutation of K to glutamine (Q), Q is electrically neutral, which is equivalent to complete acetylation. Conversely, when K is mutated to arginine (R), R is electropositive, which is equivalent to not being acetylated. We mutated all the candidate acetylated lysine sites of IDH1 (from UniProt database) to arginine (R) which mimicked the deacetylated states of protein. To investigate the mechanism by which K224 acetylation might affect IDH1 activity, we recombinantly expressed and purified human wild-type IDH1 and the K224R and K224Q mutants from E. coli.

QUANTIFICATION AND STATISTICAL ANALYSIS

Results are expressed as the mean ± SD. Differences between two groups were analyzed using Student's *t* test. One-way analysis of variance (ANOVA) was used to compare three or more groups, while two-way ANOVA was used to compare differences between groups that were split by two independent categorical variables. All statistical tests were two-sided and $p < 0.05$ was considered statistically significant. Statistical analyses were performed using SPSS 20.0 software (SPSS, Chicago, IL, USA). Statistical significance is denoted as follows: *$p < 0.05$, **$p < 0.01$, ***$p < 0.001$, and ****$p < 0.0001$, while a lack of significance is represented by ''ns'' for $p > 0.05$.